New Algorithms for Designing Unimodular Sequences with Good Correlation Properties

Petre Stoica, *Fellow, IEEE*, Hao He, *Student Member, IEEE*, Jian Li, *Fellow, IEEE*

***Abstract*—Unimodular (i.e., constant modulus) sequences with good autocorrelation properties are useful in several areas, including communications and radar. The integrated sidelobe level (ISL) of the correlation function is often used to express the goodness of the correlation properties of a given sequence. In this paper, we present several cyclic algorithms for the local minimization of ISL-related metrics. These cyclic algorithms can be initialized with a good existing sequence such as a Golomb sequence, a Frank sequence or even a (pseudo)random sequence. To illustrate the performance of the proposed algorithms, we present a number of examples including the design of sequences that have virtually zero autocorrelation sidelobes in a specified lag interval, and of long sequences that could hardly be handled by means of other algorithms previously suggested in the literature.**

***Index Terms*—Waveform design, unimodular sequences, the integrated sidelobe level, the merit factor, autocorrelation, cyclic algorithms.**

I. Introduction and Problem Formulation

Let $\{x_n\}_{n=1}^N$ denote the unimodular sequence to be designed. Without introducing any restriction, we can assume that

$$|x_n| = 1, \quad n = 1, \ldots, N. \tag{1}$$

To keep this paper as concise as possible, we will limit the discussion to general unimodular sequences, but we note here that finite-alphabet unimodular sequences, such as MPSK sequences, can also be dealt with in our framework — see, however, the *Remark* following Eq. (10).

Let

$$r_k = \sum_{n=k+1}^{N} x_n x_{n-k}^* = r_{-k}^*, \quad k = 0, \ldots, N-1 \tag{2}$$

be the correlation function of $\{x_n\}_{n=1}^N$, where $(\cdot)^*$ denotes the complex conjugate for scalars and the conjugate transpose for vectors and matrices, and let

$$\text{ISL} = \sum_{k=1}^{N-1} |r_k|^2 \tag{3}$$

be the integrated sidelobe level (ISL) metric. The main focus of this paper is on algorithms for minimizing the ISL metric or ISL-related metrics, over the set of unimodular sequences. Note that the minimization of the ISL metric is equivalent to the maximization of the merit factor (MF) defined as follows:

$$\text{MF} = \frac{|r_0|^2}{\sum\limits_{\substack{k=-(N-1)\\k\neq 0}}^{N-1} |r_k|^2} = \frac{N^2}{2\ \text{ISL}}. \tag{4}$$

Unimodular sequences with large MF values are desired in many applications, including wireless communications and range compression radar and sonar. In these applications, an emitted (probing or training) sequence with a large MF reduces the risk that the received sequence of interest is drawn in correlated multipath or clutter interferences. Additionally, the limitations of the sequence generation hardware (including the A/D conversion parts) lead to the requirement that the emitted sequence be unimodular.

Owing to the significant theoretical and practical interest in the design of unimodular sequences with good correlation properties (in particular, with large MF values), it should come as no surprise that the literature on this topic is extensive, see [1] –[21] and the many references therein.

Because the ISL metric may be highly multimodal (i.e, it may have multiple local minima), stochastic optimization algorithms have been suggested for its minimization. However, the computational burden of these algorithms becomes prohibitive as N increases: such algorithms are hardly effective on the currently available computing machines for $N \sim 10^3$ or larger. Optimization algorithms for locally minimizing the ISL metric have also been proposed. These algorithms can be used to provide quick solutions to the problem of reducing the ISL value of a given reasonably good sequence. They can also be used as local minimization blocks of a stochastic global optimization algorithm. However, most of the existing local minimization algorithms for the ISL metric are descent gradient methods whose convergence problems as well as computational burdens increase significantly as N increases.

In this paper, we introduce several cyclic algorithms (CA) for the local minimization of ISL-related metrics. The first algorithm is an extension of the CA in [21] (see also [19]

This work was supported in part by the Swedish Research Council (VR), the European Research Council (ERC), the Office of Naval Research (ONR) under Grants No. N00014-07-1-0193 and N00014-07-1-0293, the Army Research Office (ARO) under Grant No. W911NF-07-1-0450, and the National Science Foundation (NSF) under Grant No. CCF-0634786. Opinions, interpretations, conclusions, and recommendations are those of the authors and are not necessarily endorsed by the United States Government.

Petre Stoica is with the Department of Information Technology, Uppsala University, Uppsala, Sweden. Phone: 46-18-471-7619; Fax: 46-18-511925; Email: ps@it.uu.se.

Hao He is with the Department of Electrical and Computer Engineering, University of Florida, Gainesville, FL 32611-6130, USA. Email: haohe@ufl.edu.

Jian Li is with the Department of Electrical and Computer Engineering, University of Florida, Gainesville, FL 32611-6130, USA. Phone: (352) 392-2642; Fax: (352) 392-0044; Email: li@dsp.ufl.edu. Please address all correspondence to Jian Li.

and [20]), which we call CA-pruned (CAP). CAP deals with a weighted ISL (WISL) metric of the form

$$\begin{aligned} \text{WISL} = \sum_{k=1}^{N-1} w_k |r_k|^2, \\ w_k \geq 0, \quad k = 1, \ldots, N-1, \end{aligned} \tag{5}$$

corresponding to a particular set of weights $\{w_k\}_{k=1}^{N-1}$ (see Section II for details). Such weighted ISL metrics are important in applications where we want to reduce, as much as possible, the interference due to a known multipath or a known clutter discrete. CAP requires the singular value decomposition (SVD) of a matrix of dimension on the order of N, so it might be difficult to run on a PC for values of N much larger than $N \sim 10^3$. With this problem of CAP in mind, we introduce a new CA called CAN (CA-new) that can be used for the local minimization of the unweighted ISL metric (i.e., Eq. (5) with $w_k \equiv 1$). CAN is based on FFT operations and can be used virtually for any practically relevant values of N up to $N \sim 10^6$ or even larger. We also modify CAN so that it can tackle arbitrary weights, i.e., $\{w_k\}_{k=1}^{N-1}$ in Eq. (5) can be chosen as any non-negative real numbers. The resulting algorithm, which is called WeCAN (weighted CAN), requires N times more computations than CAN and it can be run on a PC for N up to $N \sim 10^4$.

II. CAP

Let

$$\mathbf{X} = \begin{bmatrix} x_1 & & 0 \\ \vdots & \ddots & \\ x_N & & x_1 \\ & \ddots & \vdots \\ 0 & & x_N \end{bmatrix}_{(2N-1)\times N} \tag{6}$$

and observe that

$$\mathbf{X}^*\mathbf{X} = \begin{bmatrix} r_0 & r_1^* & \cdots & r_{N-1}^* \\ r_1 & r_0 & \ddots & \vdots \\ \vdots & \ddots & \ddots & r_1^* \\ r_{N-1} & \cdots & r_1 & r_0 \end{bmatrix}_{N\times N}. \tag{7}$$

Because $\mathbf{X}^*\mathbf{X} \approx N\mathbf{I}$ for a sequence with good autocorrelation properties, we can think of designing $\{x_n\}_{n=1}^N$ by minimizing the following criterion:

$$\left\| \mathbf{X}^*\mathbf{X} - N\mathbf{I} \right\|^2, \tag{8}$$

over the set of unimodular sequences; hereafter, $\|\cdot\|$ denotes the Frobenius matrix norm. However, the above criterion is a quartic function of $\{x_n\}$ that is relatively difficult to tackle. With this fact in mind, the paper [21] (see also [19] and [20]) has suggested replacing Eq. (8) with the following simpler criterion (which is a quadratic function of the unknowns):

$$\left\| \mathbf{X} - \sqrt{N}\mathbf{Q} \right\|^2, \tag{9}$$

where $\mathbf{Q}$ is a $(2N-1)\times N$ semi-unitary matrix (i.e., $\mathbf{Q}^*\mathbf{Q} = \mathbf{I}$). The design problem associated with Eq. (9) can be stated as follows:

$$\begin{aligned} \min_{\{x_n\}_{n=1}^N; \mathbf{Q}} \ & \left\| \mathbf{X} - \sqrt{N}\mathbf{Q} \right\|^2 \\ \text{s.t. } & \mathbf{Q}^*\mathbf{Q} = \mathbf{I} \\ & |x_n| = 1, \quad n = 1, \ldots, N. \end{aligned} \tag{10}$$

Note that the problems of minimizing Eq. (8) and, respectively, Eq. (9) are not equivalent (these two problems may well have different solutions $\{x_n\}$), yet they are "almost equivalent" in the sense that if the criterion in Eq. (9) takes on a small value, then so does Eq. (8), and vice versa. More specifically, it is clear that Eq. (8) is equal to zero if and only if Eq. (9) is equal to zero. Consequently, by continuity arguments, if the global minimum value of Eq. (8) is "sufficiently small", then the sequences minimizing Eq. (8) and, respectively, Eq. (9) can be expected to be close to one another. Put differently, in such a case the sequence minimizing Eq. (8) leads to a small value of Eq. (9), and vice versa. However, as already mentioned, the two sequences that minimize Eq. (8) and, respectively, Eq. (9) will in general be different from one another. Furthermore, the local minima of the two criteria will in general be different; in particular they can occur at sequences that are not the same for Eq. (8) and for Eq. (9). A more quantitative mathematical analysis of the global and local minima of the two criteria, as well as of the way in which they relate to each other, appears to be a difficult task that falls beyond the scope of this paper.

Remark: As already pointed out in Section I, the case of finite-alphabet sequences can also be dealt with in our framework. However, the performance of the resulting algorithms might not be as satisfactory as that corresponding to the general unimodular case. One possible explanation of this fact is related to the above discussion on Eq. (8) and (9): when we add more constraints on $\{x_n\}$, such as a finite alphabet requirement, the minimum value of the criterion in Eq. (8) may increase quite a bit and therefore the "almost equivalence" between Eq. (8) and (9) may cease to hold true. Another explanation might be that the number of local minima of the ISL (or WISL) metric tends to increase as more constraints are imposed on $\{x_n\}$ (with the binary case being the most constrained one). Consequently, it becomes more difficult to find a sequence $\{x_n\}$ such that the criterion in Eq. (8) or (9) takes on a small value when a finite-alphabet constraint is enforced. ■

In contrast to Eq. (8), the derivation of a CA for Eq. (10) is relatively straightforward ([19]–[21]). However, this is not to say that the derivation of a CA for the criterion in Eq. (8) is infeasible. In fact such a CA can be derived, as we show in the forthcoming paper [22] that deals with *vector* sequence design. The problem with such an algorithm for Eq. (8) is that, due to the more complicated form of the criterion, it is often much slower than a CA for the "almost equivalent" criterion in Eq. (10).

We will not discuss explicitly a CA for Eq. (10) because it considers all correlation lags $\{r_k\}_{k=0}^{N-1}$, which is somewhat infrequently required in applications and therefore results in an

unnecessary increase of the computational burden. Indeed, in many cases the maximum difference between the arrival times of the sequence of interest and of the interferences is (much) smaller than the duration of the emitted sequence (see, e.g., [16][17][21][23]). Consequently, in such cases the interest lies in making $\{|r_k|\}_{k=1}^{P-1}$ small, for some $P < N$, instead of trying to make all correlation sidelobes $\{|r_k|\}_{k=1}^{N-1}$ small; here the value of P is selected based on a priori knowledge about the application at hand (for instance, in wireless communications it is usually known that significant channel tap coefficients can occur up to a certain maximum delay, and so we can choose P as the said delay). More generally, we may have a priori information that not even all $\{|r_k|\}_{k=1}^{P-1}$, but only some of them, need to be made small. In such a case, instead of considering the "all-lag" $\mathbf{X}$ in Eq. (6), we consider the following "pruned" matrix:

$$\tilde{\mathbf{X}} = \bar{\mathbf{X}}\mathbf{T} \tag{11}$$

of dimension $(N+P-1) \times Q$, where $Q \leq P \leq N$ and $\bar{\mathbf{X}}$ is a truncated version of the $\mathbf{X}$ in Eq. (6)

$$\bar{\mathbf{X}} = \begin{bmatrix} x_1 & & 0 \\ \vdots & \ddots & \\ \vdots & & x_1 \\ x_N & & \vdots \\ & \ddots & \vdots \\ 0 & & x_N \end{bmatrix}_{(N+P-1)\times P}, \tag{12}$$

and where the $P \times Q$ matrix $\mathbf{T}$ is made from Q selected columns of the $P \times P$ identity matrix, for example,

$$\mathbf{T} = \begin{bmatrix} 1 & & 0 & & & 0 \\ & \ddots & & & & \\ 0 & & 1 & 0 & & \\ & & & \vdots & & \\ & & & 1 & & 0 \\ & & & & \ddots & \\ 0 & & & 0 & & 1 \end{bmatrix}_{P\times Q}. \tag{13}$$

The above Q columns correspond to the Q correlations of interest chosen from $r_0, r_1, \ldots, r_{P-1}$. With the above notation, the design problem of interest is obtained by modifying Eq. (10) as follows:

$$\begin{aligned} \min_{\{x_n\}_{n=1}^N; \mathbf{U}} & \left\| \tilde{\mathbf{X}} - \sqrt{N}\mathbf{U} \right\|^2 \\ \text{s.t. } & \mathbf{U}^*\mathbf{U} = \mathbf{I} \\ & |x_n| = 1, \quad n = 1, \ldots, N, \end{aligned} \tag{14}$$

where $\mathbf{U}$ is an $(N+P-1) \times Q$ semi-unitary matrix.

Remark: Eq. (14) is "almost equivalent" to minimizing $\|\tilde{\mathbf{X}}^*\tilde{\mathbf{X}} - N\mathbf{I}\|^2$. When $Q = P$, we have

$$\tilde{\mathbf{X}}^*\tilde{\mathbf{X}} = \begin{bmatrix} r_0 & r_1^* & \cdots & r_{P-1}^* \\ r_1 & r_0 & \ddots & \vdots \\ \vdots & \ddots & \ddots & r_1^* \\ r_{P-1} & \cdots & r_1 & r_0 \end{bmatrix}_{P\times P}, \tag{15}$$

which shows that in this case CAP implicitly assumes the weight of $w_k = 2(P-k)$ for r_k $(k = 1, \ldots, P-1)$ in the WISL metric in Eq. (5), and 0 weights for the other correlation lags. When $Q < P$, $\tilde{\mathbf{X}}^*\tilde{\mathbf{X}}$ is no longer a Toeplitz matrix and a general expression for w_k does not exist anymore. Roughly speaking, the number of times that r_k (together with r_k^*) appears in the matrix $\tilde{\mathbf{X}}^*\tilde{\mathbf{X}}$ determines the corresponding weight w_k. ■

Regarding the minimization problem in Eq. (14), we note the following facts. For given $\tilde{\mathbf{X}}$, let

$$\tilde{\mathbf{X}}^* = \mathbf{U}_1\mathbf{\Sigma}\mathbf{U}_2^* \tag{16}$$

denote the SVD of $\tilde{\mathbf{X}}^*$ (here $\mathbf{U}_1$ is a $Q \times Q$ unitary matrix, $\mathbf{U}_2$ is a $(N+P-1) \times Q$ semi-unitary matrix, and $\mathbf{\Sigma}$ is a $Q \times Q$ diagonal matrix). Then the solution $\mathbf{U}$ of Eq. (14), for fixed $\tilde{\mathbf{X}}$, is given by (see [19] or the references there and in [20]):

$$\mathbf{U} = \mathbf{U}_2\mathbf{U}_1^*. \tag{17}$$

Next note that, for given $\mathbf{U}$, the minimization of Eq. (14) with respect to $\{x_n\}_{n=1}^N$ also has a simple closed-form solution. To see this, let x denote an arbitrary element of the sequence $\{x_n\}_{n=1}^N$. Then it follows from Eq. (14) that the generic form of the minimization problem with respect to the elements of $\{x_n\}_{n=1}^N$ is:

$$\min_x \sum_{k=1}^{Q} |x - \mu_k|^2, \tag{18}$$

where $\{\mu_k\}_{k=1}^Q$ are the elements of the matrix $\sqrt{N}\mathbf{U}$ whose positions are the same as the positions of x in $\tilde{\mathbf{X}}$. (As an example, let us assume that $Q = P$ and therefore that $\tilde{\mathbf{X}} = \bar{\mathbf{X}}$. Then, for $x = x_n$, the corresponding sequence $\{\mu_k\}_{k=1}^P$ is given by the $(n-1+i, i)^{\text{th}}$-elements of $\sqrt{N}\mathbf{U}$, for $i = 1, \ldots, P$.) Because $|x| = 1$, the criterion in Eq. (18) can be rewritten as:

$$\begin{aligned} \sum_{k=1}^{Q} |x - \mu_k|^2 &= \text{ const} - 2\text{Re}\left[x \sum_{k=1}^{Q} \mu_k^* \right] \\ &= \text{const} - 2\left| \sum_{k=1}^{Q} \mu_k \right| \cdot \cos\left[\arg(x) - \arg(\sum_{k=1}^{Q} \mu_k) \right]. \end{aligned} \tag{19}$$

Hence the minimizer x of the criterion in Eq. (18) is given by

$$x = e^{j\phi}, \quad \phi = \arg(\sum_{k=1}^{Q} \mu_k). \tag{20}$$

The CAP for the cyclic minimization of the criterion in Eq. (14) follows from the above discussion as a natural corollary:

CAP

- Step 0
  Set the matrix $\tilde{\mathbf{X}}$ to an initial value (e.g., $\{x_n\}_{n=1}^N$ can be set to $\{e^{j2\pi\theta_n}\}_{n=1}^N$ where $\{\theta_n\}_{n=1}^N$ are independent random variables uniformly distributed in $[0, 2\pi]$, or $\{x_n\}_{n=1}^N$ can be initialized by a good existing sequence such as a Golomb sequence [12]).
- Step 1
  Compute the semi-unitary matrix $\mathbf{U}$ that minimizes Eq. (14) for $\{x_n\}_{n=1}^N$ fixed at its most recent value (see Eqs. (16) and (17)).
- Step 2
  Compute the sequence $\{x_n\}_{n=1}^N$ that minimizes Eq. (14), under the constraint $|x_n| = 1$, for $\mathbf{U}$ fixed at its most recent value (see Eq. (20)).
- Iteration
  Repeat Steps 1 and 2 until some stop criterion is satisfied e.g. $\|\mathbf{x}^{(i)} - \mathbf{x}^{(i+1)}\| < \epsilon$, where $\mathbf{x}^{(i)}$ is the sequence obtained at the i^{th} iteration, and ϵ is a predefined threshold (see the *Remark* in Section V-C for a brief discussion about how to choose the value of ϵ).

The SVD of the $Q \times (N + P - 1)$ matrix $\tilde{\mathbf{X}}^*$ in Eq. (16) is relatively computationally intensive for large values of N and Q. As a rough rule of thumb, on a regular PC the use of CAP may be limited to values of $N \sim 10^3$ depending on how many correlation lags are considered. In the next section, we introduce a new CA (CAN = CA-new) for the local minimization of the unweighted ISL metric that does not have such a limitation: indeed CAN can be used with values of $N \sim 10^6$ or even larger if so desired.

III. CAN

The derivation of CAN involves several steps, the first of which consists of expressing the ISL metric in the frequency domain. It is well known that, for any $\omega \in [0, 2\pi]$,

$$\left|\sum_{n=1}^{N} x_n e^{-j\omega n}\right|^2 = \sum_{k=-(N-1)}^{N-1} r_k e^{-j\omega k} \triangleq \Phi(\omega) \tag{21}$$

(see, e.g., [24]). Furthermore, it can be shown that the ISL metric in Eq. (3) can be equivalently written as:

$$\text{ISL} = \frac{1}{4N}\sum_{p=1}^{2N}\left[\Phi(\omega_p) - N\right]^2, \tag{22}$$

where $\{\omega_p\}$ are the following Fourier frequencies:

$$\omega_p = \frac{2\pi}{2N}p, \quad p = 1, \ldots, 2N. \tag{23}$$

(Note that Eq. (22) is a Parseval-type equality.) To prove Eq. (22), let δ_k denote the Kronecker delta:

$$\delta_k = \begin{cases} 1, & \text{for } k = 0 \\ 0, & \text{for } k \neq 0, \end{cases}$$

and use the correlogram-based expression for $\Phi(\omega)$ in Eq. (21) to verify that:

$$\begin{aligned}\sum_{p=1}^{2N}\left[\Phi(\omega_p) - N\right]^2 &= \sum_{p=1}^{2N}\left[\sum_{k=-(N-1)}^{N-1}(r_k - N\delta_k)e^{-j\omega_p k}\right]^2 \\ &= \sum_{k=-(N-1)}^{N-1}\sum_{\tilde{k}=-(N-1)}^{N-1}(r_k - N\delta_k)(r_{\tilde{k}} - N\delta_{\tilde{k}})^* \\ &\qquad \left[\sum_{p=1}^{2N} e^{-j\omega_p(k-\tilde{k})}\right]. \end{aligned} \tag{24}$$

Because, for $|k - \tilde{k}| \leq 2N - 2$,

$$\begin{aligned}\sum_{p=1}^{2N} e^{-j\omega_p(k-\tilde{k})} &= e^{-j\frac{2\pi}{2N}(k-\tilde{k})} \cdot \frac{e^{-j2\pi(k-\tilde{k})} - 1}{e^{-j\frac{2\pi}{2N}(k-\tilde{k})} - 1} \\ &= 2N\delta_{(k-\tilde{k})}, \end{aligned} \tag{25}$$

we obtain from Eq. (24) the following equation:

$$\begin{aligned}\frac{1}{4N}\sum_{p=1}^{2N}\left[\Phi(\omega_p) - N\right]^2 &= \frac{1}{2}\sum_{k=-(N-1)}^{N-1}|r_k - N\delta_k|^2 \\ &= \sum_{k=1}^{N-1}|r_k|^2 = \text{ISL}, \end{aligned} \tag{26}$$

which is Eq. (22). Using the periodogram-based expression for $\Phi(\omega)$ (see Eq. (21)) in Eq. (22) shows that the problem of minimizing the ISL is equivalent to the minimization of the following frequency-domain metric:

$$\sum_{p=1}^{2N}\left[\left|\sum_{n=1}^{N} x_n e^{-j\omega_p n}\right|^2 - N\right]^2. \tag{27}$$

This equivalence result has an obvious intuitive interpretation: minimizing the ISL makes the sequence behave like white noise, and consequently its periodogram should be nearly constant in frequency.

The next point to note is that the criterion in Eq. (27) is a quartic function of $\{x_n\}$. However, using the same type of argument as the one that led from Eq. (8) to Eq. (9), we can readily verify that the minimization of Eq. (27) with respect to $\{x_n\}$ is "almost equivalent" to the following simpler problem (whose criterion is a quadratic function of $\{x_n\}$):

$$\min_{\{x_n\}_{n=1}^N;\{\psi_p\}_{p=1}^{2N}} \sum_{p=1}^{2N}\left|\sum_{n=1}^{N} x_n e^{-j\omega_p n} - \sqrt{N}e^{j\psi_p}\right|^2. \tag{28}$$

Let

$$\mathbf{a}_p^* = \begin{bmatrix} e^{-j\omega_p} & \cdots & e^{-j2N\omega_p} \end{bmatrix}, \tag{29}$$

let $\mathbf{A}^*$ be the following unitary $2N \times 2N$ FFT matrix:

$$\mathbf{A}^* = \frac{1}{\sqrt{2N}}\begin{bmatrix} \mathbf{a}_1^* \\ \vdots \\ \mathbf{a}_{2N}^* \end{bmatrix}, \tag{30}$$

and let $\mathbf{z}$ be the sequence $\{x_n\}_{n=1}^N$ padded with N zeros:

$$\mathbf{z} = \begin{bmatrix} x_1 & \cdots & x_N & 0 & \cdots & 0 \end{bmatrix}_{2N\times 1}^T. \tag{31}$$

Then the criterion in Eq. (28) can be rewritten in the following more compact form (to within a multiplicative constant):

$$\|\mathbf{A}^*\mathbf{z} - \mathbf{v}\|^2, \tag{32}$$

where

$$\mathbf{v} = \frac{1}{\sqrt{2}} \begin{bmatrix} e^{j\psi_1} & \cdots & e^{j\psi_{2N}} \end{bmatrix}^T. \tag{33}$$

For given $\{x_n\}$, the minimization of Eq. (32) with respect to $\{\psi_p\}$ is immediate: let

$$\mathbf{f} = \mathbf{A}^*\mathbf{z} \tag{34}$$

denote the FFT of $\mathbf{z}$; then

$$\psi_p = \arg(f_p), \quad p = 1, \ldots, 2N. \tag{35}$$

Similarly, for given $\mathbf{v}$, let

$$\mathbf{g} = \mathbf{A}\mathbf{v} \tag{36}$$

denote the IFFT of $\mathbf{v}$. Because $\|\mathbf{A}^*\mathbf{z} - \mathbf{v}\|^2 = \|\mathbf{z} - \mathbf{A}\mathbf{v}\|^2$, it follows that the minimizing sequence $\{x_n\}$ is given by:

$$x_n = e^{j\arg(g_n)}, \quad n = 1, \ldots, N. \tag{37}$$

The CAN for the cyclic local minimization of the ISL-related metric in Eq. (28) can now be summarized as follows:

CAN

- Step 0
  Set the $\{x_n\}_{n=1}^N$ to some initial values (e.g., $\{x_n\}_{n=1}^N$ can be randomly generated or given by a good existing sequence, as mentioned in the CAP algorithm in Section II).
- Step 1
  Compute the $\{\psi_p\}_{p=1}^{2N}$ that minimize the metric for $\{x_n\}_{n=1}^N$ fixed at their most recent values (see Eq. (35)).
- Step 2
  Compute the sequence $\{x_n\}_{n=1}^N$ that minimizes the metric, under the constraint $|x_n| = 1$, for $\{\psi_p\}_{p=1}^{2N}$ fixed at their most recent values (see Eq. (37)).
- Iteration
  Repeat Steps 1 and 2 until a pre-specified stop criterion is satisfied e.g. $\|\mathbf{x}^{(i)} - \mathbf{x}^{(i+1)}\| < \epsilon$, where $\mathbf{x}^{(i)}$ is the sequence obtained at the i^{th} iteration, and ϵ is a predefined threshold, such as 10^{-3}.

Owing to its simple (I)FFT operations, CAN can be used for very large values of N, such as $N \sim 10^6$.

In the next section, we present an extended version of CAN which can deal with the WISL metric (with arbitrarily chosen weights) as defined in Eq. (5). The extended algorithm is called WeCAN (weighted CAN). The price paid for WeCAN's ability to deal with a general WISL metric is an increased computational burden compared to CAN. Specifically, as will be shown in the next section, each iteration of WeCAN requires N computations of $2N$-point (I)FFT's; thus the number of flops required by WeCAN is roughly N times larger than that of CAN. Nonetheless, WeCAN can still be used for relatively large values of N, such as $N \sim 10^4$.

IV. WeCAN

Similarly to the proof of Eq. (22) in Section III, we can derive the following expression for the WISL metric (γ_k below is related to the weight w_k in Eq. (5) as $w_k = \gamma_k^2$):

$$\text{WISL} = \sum_{k=1}^{N-1} \gamma_k^2 |r_k|^2 \tag{38}$$

$$= \frac{1}{4N} \sum_{p=1}^{2N} [\tilde{\Phi}(\omega_p) - \gamma_0 N]^2, \tag{39}$$

where

$$\tilde{\Phi}(\omega_p) \stackrel{\triangle}{=} \sum_{k=-(N-1)}^{N-1} \gamma_k r_k e^{-j\omega_p k}, \tag{40}$$

$$\omega_p = \frac{2\pi}{2N} p, \quad p = 1, \ldots, 2N,$$

and where $\{\gamma_k\}_{k=1}^{N-1}$ are real-valued (with $\gamma_k = \gamma_{-k}$). Note that by choosing $\{\gamma_k\}_{k=1}^{N-1}$ appropriately, we can weigh the correlation lags in Eq. (38) in any desired way. Regarding γ_0, which does not enter into Eq. (38), it will be chosen to ensure that the matrix

$$\mathbf{\Gamma} = \frac{1}{\gamma_0} \begin{bmatrix} \gamma_0 & \gamma_1 & \cdots & \gamma_{N-1} \\ \gamma_1 & \gamma_0 & \ddots & \vdots \\ \vdots & \ddots & \ddots & \gamma_1 \\ \gamma_{N-1} & \cdots & \gamma_1 & \gamma_0 \end{bmatrix} \tag{41}$$

is positive semi-definite, which we denote by $\mathbf{\Gamma} \geq 0$. This can be done in the following simple way: let $\tilde{\mathbf{\Gamma}}$ be the matrix $\gamma_0\mathbf{\Gamma}$ with all diagonal elements set to 0, and let $\lambda_{\min}$ denote the minimum eigenvalue of $\tilde{\mathbf{\Gamma}}$; then $\mathbf{\Gamma} \geq 0$ if and only if $\gamma_0 + \lambda_{\min} \geq 0$, a condition that can always be satisfied by selecting γ_0.

Next we will derive a criterion that is "almost equivalent" to Eq. (39) and which depends quadratically on the unknowns $\{x_n\}_{n=1}^N$, similarly to what we have done in the previous sections. To do so, we must apparently obtain a square root of $\tilde{\Phi}(\omega_p)$ in Eq. (40) that is linear in $\{x_n\}_{n=1}^N$. Note the following DFT pairs:

$$\{r_k\} \longleftrightarrow \Phi(\omega) = |X(\omega)|^2$$
$$\{\gamma_k r_k\} \longleftrightarrow \tilde{\Phi}(\omega) = \Gamma(\omega) * |X(\omega)|^2, \tag{42}$$

where

$$X(\omega) = \sum_{n=1}^{N} x_n e^{-jn\omega}, \quad \Gamma(\omega) = \sum_{k=-(N-1)}^{N-1} \gamma_k e^{-j\omega k}, \tag{43}$$

and where $*$ is the convolution operator. Thus $\tilde{\Phi}(\omega_p)$ can be expressed as

$$\tilde{\Phi}(\omega_p) = \frac{1}{2\pi} \int_{-\pi}^{\pi} \Gamma(\omega_p - \psi) |X(\psi)|^2 \, d\psi \tag{44}$$

$$= \frac{1}{2\pi} \int_{-\pi}^{\pi} \sum_{k=-(N-1)}^{N-1} \gamma_k e^{-jk(\omega_p - \psi)} \sum_{n=1}^{N} x_n e^{-jn\psi} \sum_{\tilde{n}=1}^{N} x_{\tilde{n}}^* e^{j\tilde{n}\psi} d\psi$$

$$= \sum_{k=-(N-1)}^{N-1} \sum_{n=1}^{N} \sum_{\tilde{n}=1}^{N} \gamma_k x_n x_{\tilde{n}}^* \left\{ \frac{1}{2\pi} \int_{-\pi}^{\pi} e^{j\psi(k-n+\tilde{n})} d\psi \right\} e^{-j\omega_p k}.$$

It is easy to verify that

$$\frac{1}{2\pi}\int_{-\pi}^{\pi} e^{j\psi(k-n+\tilde{n})}\ d\psi = \delta_{k-(n-\tilde{n})}. \tag{45}$$

Thus

$$\begin{aligned}\tilde{\Phi}(\omega_p) &= \sum_{n=1}^{N}\sum_{\tilde{n}=1}^{N}\gamma_{n-\tilde{n}}x_n x_{\tilde{n}}^* e^{-j\omega_p(n-\tilde{n})} \\ &= \tilde{\mathbf{x}}_p^*(\gamma_0\mathbf{\Gamma})\tilde{\mathbf{x}}_p,\end{aligned} \tag{46}$$

where

$$\tilde{\mathbf{x}}_p = \begin{bmatrix} x_1 e^{-j\omega_p} & x_2 e^{-j2\omega_p} & \cdots & x_N e^{-jN\omega_p}\end{bmatrix}^T \tag{47}$$

and $\mathbf{\Gamma}$ is defined in Eq. (41). Therefore the WISL metric in Eq. (39) can be written as

$$\text{WISL} = \frac{\gamma_0^2}{4N}\sum_{p=1}^{2N}\left[\tilde{\mathbf{x}}_p^*\mathbf{\Gamma}\tilde{\mathbf{x}}_p - N\right]^2. \tag{48}$$

This expression suggests that the following problem can be expected to be "almost equivalent" to the minimization of the WISL metric:

$$\begin{aligned}\min_{\{x_n\}_{n=1}^N,\{\boldsymbol{\alpha}_p\}_{p=1}^{2N}} &\sum_{p=1}^{2N}\|\mathbf{C}\tilde{\mathbf{x}}_p - \boldsymbol{\alpha}_p\|^2 \\ \text{s.t. } &\|\boldsymbol{\alpha}_p\|^2 = N, \quad p = 1,\ldots,2N, \\ &|x_n| = 1, \quad n = 1,\ldots,N,\end{aligned} \tag{49}$$

where the $N \times N$ matrix $\mathbf{C}$ is a square root of $\mathbf{\Gamma}$, i.e., $\mathbf{\Gamma} = \mathbf{C}^T\mathbf{C}$.

A cyclic algorithm for Eq. (49), which we will call WeCAN, can be derived as follows. For given $\{x_n\}_{n=1}^N$, Eq. (49) decouples into $2N$ independent problems each of which has the following form:

$$\begin{aligned}\min_{\boldsymbol{\alpha}_p} &\|\mathbf{f}_p - \boldsymbol{\alpha}_p\|^2 \\ \text{s.t. } &\|\boldsymbol{\alpha}_p\|^2 = N\end{aligned} \tag{50}$$

where the $N \times 1$ vector $\mathbf{f}_p = \mathbf{C}\tilde{\mathbf{x}}_p$ is given. Note that under the constraint $\|\boldsymbol{\alpha}_p\|^2 = N$ we have

$$\begin{aligned}\|\mathbf{f}_p - \boldsymbol{\alpha}_p\|^2 &= \text{ const } - 2\ \text{Re}\{\mathbf{f}_p^*\boldsymbol{\alpha}_p\} \\ &\geq \text{ const } - 2\|\mathbf{f}_p\|\|\boldsymbol{\alpha}_p\| = \text{ const } - 2N\|\mathbf{f}_p\|,\end{aligned} \tag{51}$$

where the equality is achieved if and only if

$$\boldsymbol{\alpha}_p = \sqrt{N}\frac{\mathbf{f}_p}{\|\mathbf{f}_p\|}. \tag{52}$$

This is therefore the solution to the minimization problem in Eq. (49) for given $\{x_n\}_{n=1}^N$. Note that the computation of $\{\mathbf{f}_p\}_{p=1}^{2N}$ can be done by means of the FFT. Indeed, let c_{kn} denote the $(k,n)^{\text{th}}$ element of $\mathbf{C}$ and define

$$\mathbf{z}_k = \begin{bmatrix} c_{k1}x_1 & \cdots & c_{kN}x_N & 0 & \cdots & 0\end{bmatrix}_{(2N\times 1)}^T \tag{53}$$

and

$$\mathbf{F} = \sqrt{2N}\mathbf{A}^* \cdot \begin{bmatrix}\mathbf{z}_1 & \mathbf{z}_2 & \cdots \mathbf{z}_N\end{bmatrix}_{2N\times N} \tag{54}$$

where the unitary $2N \times 2N$ FFT matrix $\mathbf{A}^*$ has been defined in Eq. (30). Then it is not difficult to see that the transpose of the vector $\mathbf{f}_p$ is given by the p^{th} row of $\mathbf{F}$.

Next we show that, for given $\{\boldsymbol{\alpha}_p\}_{p=1}^{2N}$, the minimization problem in Eq. (49) with respect to $\{x_n\}_{n=1}^N$ also has a closed-form solution. Let α_{pk} denote the k^{th} element of $\boldsymbol{\alpha}_p$ and let $\mathbf{a}_p^*$ be given by Eq. (29). Using this notation, the criterion in Eq. (49) can be written as

$$\begin{aligned}\sum_{p=1}^{2N}\|\mathbf{C}\tilde{\mathbf{x}}_p - \boldsymbol{\alpha}_p\|^2 &= \sum_{k=1}^{N}\sum_{p=1}^{2N}\left|\mathbf{a}_p^*\mathbf{z}_k - \alpha_{pk}\right|^2 \\ &= \sum_{k=1}^{N}\|\mathbf{A}^*\mathbf{z}_k - \boldsymbol{\beta}_k\|^2 = \sum_{k=1}^{N}\|\mathbf{z}_k - \mathbf{A}\boldsymbol{\beta}_k\|^2,\end{aligned} \tag{55}$$

where

$$\boldsymbol{\beta}_k = \frac{1}{\sqrt{2N}}\begin{bmatrix}\alpha_{1k} & \cdots & \alpha_{2N,k}\end{bmatrix}^T, \quad k = 1,\ldots,N. \tag{56}$$

For a generic element of $\{x_n\}_{n=1}^N$, denoted as x, Eq. (55) becomes

$$\sum_{k=1}^{N}|\mu_k x - \nu_k|^2 = \text{ const } - 2\ \text{Re}\left[\left(\sum_{k=1}^{N}\mu_k^*\nu_k\right)x^*\right], \tag{57}$$

where μ_k and ν_k are given by the corresponding elements in $\mathbf{z}_k$ and $\mathbf{A}\boldsymbol{\beta}_k$, respectively. Under the unimodular constraint, the minimizer x of the criterion in Eq. (57) is given by

$$x = e^{j\phi}, \quad \phi = \arg\left(\sum_{k=1}^{N}\mu_k^*\nu_k\right). \tag{58}$$

This observation concludes the derivation of the main steps of the WeCAN algorithm, whose summary is as follows:

WeCAN

- Step 0
  Set the $\{x_n\}_{n=1}^N$ to some initial values and select the desired weights $\{\gamma_k\}_{k=1}^{N-1}$; also choose γ_0 such that the matrix $\mathbf{\Gamma}$ in Eq. (41) is positive semidefinite.
- Step 1
  Compute the $\{\boldsymbol{\alpha}_p\}_{p=1}^{2N}$ that minimize the criterion in Eq. (49) for $\{x_n\}_{n=1}^N$ fixed at their most recent values (see Eq. (52)).
- Step 2
  Compute the sequence $\{x_n\}_{n=1}^N$ that minimizes the criterion in Eq. (49) for $\{\boldsymbol{\alpha}_p\}_{p=1}^{2N}$ fixed at their most recent values (see Eq. (58)).
- Iteration
  Repeat Steps 1 and 2 until a pre-specified stop criterion is satisfied (see the CAP algorithm in Section II).

In the case of non-uniform weighting, we define the modified merit factor (MMF) using the weighted ISL as follows:

$$\text{MMF} = \frac{|r_0|^2}{2\text{WISL}} = \frac{N^2}{2\sum_{k=1}^{N-1}w_k|r_k|^2}. \tag{59}$$

We have observed empirically that WeCAN increases the MMF systematically when initialized by CAP, and vice versa. This motivates us to use CAP to initialize WeCAN, then use WeCAN to initialize CAP, and so on. The so-obtained combined iterative method is called WeCAN+CAP. As will be shown in Section V, when the maximum lag considered is smaller than half of the sequence length, WeCAN, CAP

and their combination WeCAN+CAP can generate sequences that have virtually an "infinite" MMF; the same is true even when the number of lags considered is smaller than half of the sequence length, provided the maximum lag under consideration is not too close to N (see the next section for more details on this aspect).

V. Numerical Examples

A. ISL Design

We compare the merit factors of the Golomb sequence ([12]), of the Frank sequence ([15]), and of the CAN sequence initialized by one of these two types of sequences (denoted as CAN(G) and CAN(F), respectively). A Golomb sequence $\{g(n)\}_{n=1}^{N}$ of length N is defined as

$$g(n) = e^{j\pi(n-1)n/N}, \quad n = 1, \ldots, N, \tag{60}$$

where N can be any positive integer. Frank sequences are only defined for lengths that are perfect squares. For $N = M^2$, a Frank sequence can be written as

$$f(nM + k + 1) = e^{j2\pi nk/M}, \ n, k = 0, 1, \ldots, M-1. \tag{61}$$

(Note that the above sequences can be easily computed for any value of N of possible practical interest, with the only restriction that N must be a perfect square in the case of Eq. (61).) We compute the merit factors of the above four types of sequences (Golomb, Frank, CAN(G) and CAN(F)) for the following lengths: $N = 3^2, 5^2, 10^2, 15^2, 20^2, 30^2, 70^2$ and 100^2. The results are shown in Figure 1 using a log-log scale. For all sequence lengths we consider, the CAN(G) and CAN(F) sequences give nearly the same merit factors; both are much larger than the merit factors given by the Golomb or Frank sequence. When $N = 10^4$, the CAN(G) sequence provides the largest merit factor of 1839.76, which is more than ten times larger than that given by the Golomb sequence (which is 157.10). We also show the correlation levels of the Golomb and CAN(G) sequences of lengths $N = 10^2, 10^3$ and 10^4 in Figure 2. The correlation level is defined as

$$\text{correlation level} = 20\log_{10}\left|\frac{r_k}{r_0}\right|, \quad k = 1, \ldots, N-1. \tag{62}$$

We note that the correlation sidelobes of the Golomb sequence are comparatively large for k close to 0 and $N-1$ (the same is true for the Frank sequence), while the CAN(G) sequence has relatively more uniform correlation sidelobes as k increases from 0 to $N-1$.

B. WISL Design - A First Example

Consider the design of a data sequence of length $N = 100$. Suppose that we are interested in suppressing the correlations $r_1, \ldots, r_{25}$ and $r_{70}, \ldots, r_{79}$. Three methods are used to design the sequence. The first method is the original CA for Eq. (10), in which all correlation levels from r_1 to r_{99} are taken into account. The second method is the CAP for Eq. (14) which focuses on $r_1, \ldots, r_{25}$ and $r_{70}, \ldots, r_{79}$ and therefore uses $P = 80, Q = 36$ and the following matrix $\mathbf{T}$:

$$\mathbf{T} = \begin{bmatrix} \mathbf{I}_{26} & 0 \\ 0 & \vdots \\ \vdots & 0 \\ 0 & \mathbf{I}_{10} \end{bmatrix}_{80\times 36}, \tag{63}$$

where $\mathbf{I}_K$ denotes the $K \times K$ identity matrix. The third method is the WeCAN algorithm for Eq. (48) and (49), with the following weights used in the matrix $\mathbf{\Gamma}$ in Eq. (41):

$$\gamma_k = \begin{cases} 1, & k \in [1, 25] \cup [70, 79] \\ 0, & k \in [26, 69] \cup [80, 99] \end{cases}. \tag{64}$$

(γ_0 is chosen to ensure the positive semi-definiteness of $\mathbf{\Gamma}$; more exactly we choose $\gamma_0 = 12.05$ following the discussion right after Eq. (41).)

In this scenario, the MMF is as defined in Eq. (59) with

$$w_k = \gamma_k^2 = \begin{cases} 1, & k \in [1, 25] \cup [70, 79] \\ 0, & k \in [26, 69] \cup [80, 99] \end{cases}. \tag{65}$$

All three methods mentioned above are initialized by a randomly generated sequence (see Step 0 of the CAP algorithm in Section II). The correlation levels of the designed sequences are shown in Figure 3. The WeCAN sequence has correlation sidelobes that are practically zero at the required lags, and which are much smaller than the sidelobes of the CA or CAP sequence and those of the Golomb or CAN(G) sequence in the last subsection (see Figure 2(a) and 2(b)). Table I presents the corresponding MMF values. The MMF of the WeCAN sequence (which is practically infinite) is significantly larger than the other MMF values in the table.

TABLE I
MMF values for the weights in Eq. (65) and $N = 100$

	Golomb	CAN(G)	CA	CAP	WeCAN
MMF	32.55	142.64	68.07	229.02	1.06×10^{21}

The matrix $\tilde{\mathbf{X}}^*\tilde{\mathbf{X}}$ employed by CAP in this example (where $\tilde{\mathbf{X}}$ is given by Eq. (11)) is composed of $r_1, \ldots, r_{25}$ and $r_{70}, \ldots, r_{79}$, but also of $r_{45}, \ldots, r_{69}$. Therefore, although not of direct interest to us, $r_{45}, \ldots, r_{69}$ are minimized as well (see Figure 3(b)), which increases the difficulty of the problem. If we consider fewer correlation lags (e.g., $r_1, \ldots, r_9$ and $r_{70}, \ldots, r_{79}$ only), CAP is also able to provide practically zero correlation sidelobes at the required lags. On the other hand, if more correlation lags are taken into account, then correlation sidelobes of either CAP or WeCAN become higher; the reason is that fewer and fewer degrees of freedom of the sequence $\{x_n\}_{n=1}^{N}$ can be used to control $|r_k|$ as k increases beyond $N/2$ (in particular note that $|r_{N-1}| = 1$ can not be decreased).

C. WISL Design - A Second Example

Consider, once again, the design of a data sequence of length $N = 100$ but now with the aim of suppressing the correlations $r_1, \ldots, r_{39}$. We compare the CAP sequence and the WeCAN+CAP sequence, both obtained using random initialization. The CAP sequence is generated using $P = Q = 40$

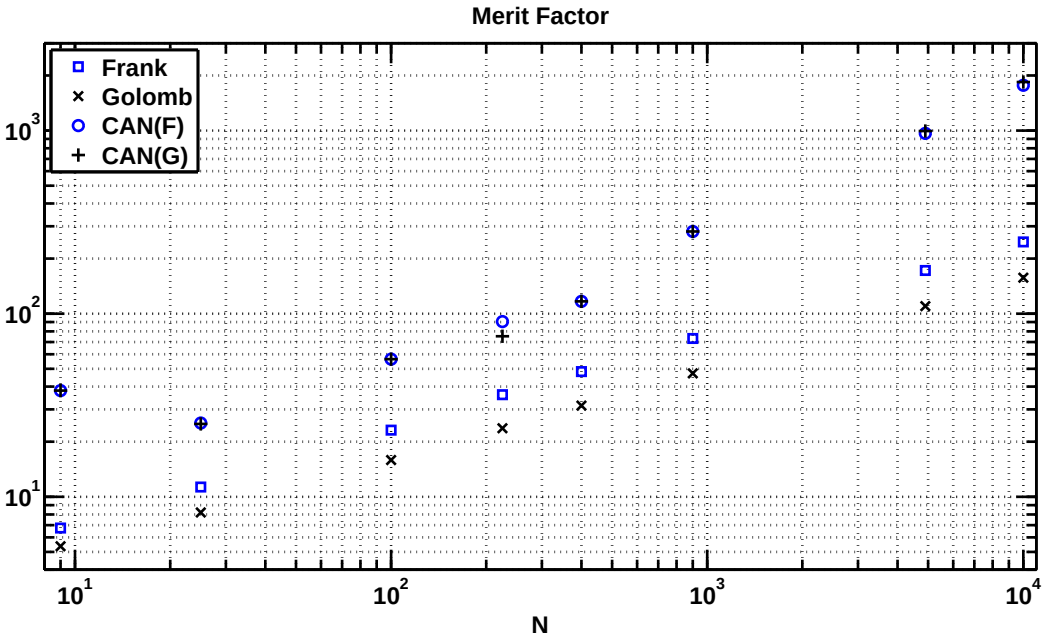

Fig. 1. The merit factors of the Golomb, Frank, CAN(G) and CAN(F) sequences of lengths from 3^2 up to 100^2.

and thus $\tilde{\mathbf{X}} = \bar{\mathbf{X}}$ in Eq. (11). The WeCAN+CAP sequence is generated as outlined at the end of Section IV. To construct the matrix $\mathbf{\Gamma}$ in Eq. (41), we define

$$\gamma_k = \begin{cases} 1, & k \in [1, 39] \\ 0, & k \in [40, 99] \end{cases}, \qquad w_k = \gamma_k^2, \quad k = 1, \ldots, 99, \tag{66}$$

and choose γ_0 such that $\mathbf{\Gamma} \geq 0$.

Figure 4 shows the correlation levels of the so-obtained CAP and WeCAN+CAP sequences, and Table II presents the corresponding MMF values (the CAN(G) sequence is included in the table for the sake of comparison). Both sequences have practically 0 correlation sidelobes from r_1 to r_{P-1}, and the corresponding MMF can be considered to be infinity (the smallest correlation level in Figure 4 is around -320dB, i.e., 10^{-16}, which is the smallest number that can be properly handled in MATLAB and can thus be considered as "zero").

A point worth mentioning here is that the CAP and WeCAN+CAP algorithms are able to provide an "infinite" MMF in this example if $P \leq 50$. The reason is that the number of degrees of freedom in this example is $N - 1 = 99$ (there are $N - 1$ free phases as the initial phase does not matter) and our goal is to match $2(P - 1)$ real numbers (i.e., the real and imaginary parts of $r_1, \ldots, r_{P-1}$). Consequently the matching is possible in principle only when $2(P - 1) \leq N - 1$, which leads to $P \leq (N + 1)/2$. In the next subsection, P is fixed to 40 and N is varied from 100 to 500, in which case the CAP or WeCAN+CAP algorithm consistently generates sequences that have an "infinite" MMF.

TABLE II
MMF VALUES FOR THE WEIGHTS IN EQ. (66) AND $N = 100$

	CAN(G)	CAP	WeCAN+CAP
MMF	126.27	1.08×10^{23}	2.37×10^{26}

Remark: The WeCAN algorithm is also able to provide an "infinite" MMF in this example, although we do not show its results here for brevity. Another fact worth pointing out is that both CAP and WeCAN algorithms require a proper value of the stop criterion parameter ϵ (see Section II) to perform well. When the number of considered correlation lags is less than $(N + 1)/2$ and N is relatively small (such as $N \sim 10^2$), a sufficiently small ϵ should be used (e.g., $\epsilon = 10^{-13}$ in the examples in this and the last subsection) to permit enough many iterations, which drive the correlation sidelobes to zero, to be run; in other cases, a "moderate" ϵ (depending on the application, such as 10^{-5}) is preferable to prevent the program from running indefinitely without suppressing the correlation sidelobes anymore. In contrast with this, WeCAN+CAP is quite insensitive to the choice of ϵ ($\epsilon = 10^{-5}$ is appropriate for WeCAN+CAP in all cases that we have tested) and it outperforms CAP in terms of MMF, especially for large values of N. ■

D. FIR Channel Estimation

Consider an FIR channel impulse response $\{h_p\}_{p=0}^{P-1}$ whose estimation is our main goal (the number of channel taps P is assumed to be known). Suppose we transmit a probing sequence $\{x_n\}_{n=1}^{N}$ and obtain the received signal

$$y_n = \sum_{p=0}^{P-1} h_p x_{n-p} + e_n, \quad n = 1, \ldots, N + P - 1, \tag{67}$$

where $\{e_n\}_{n=1}^{N+P-1}$ is an i.i.d. complex Gaussian white noise sequence with zero mean and variance σ^2. Eq. (67) can be written in the following more compact form:

$$\mathbf{y} = \bar{\mathbf{X}}\mathbf{h} + \mathbf{e} \tag{68}$$

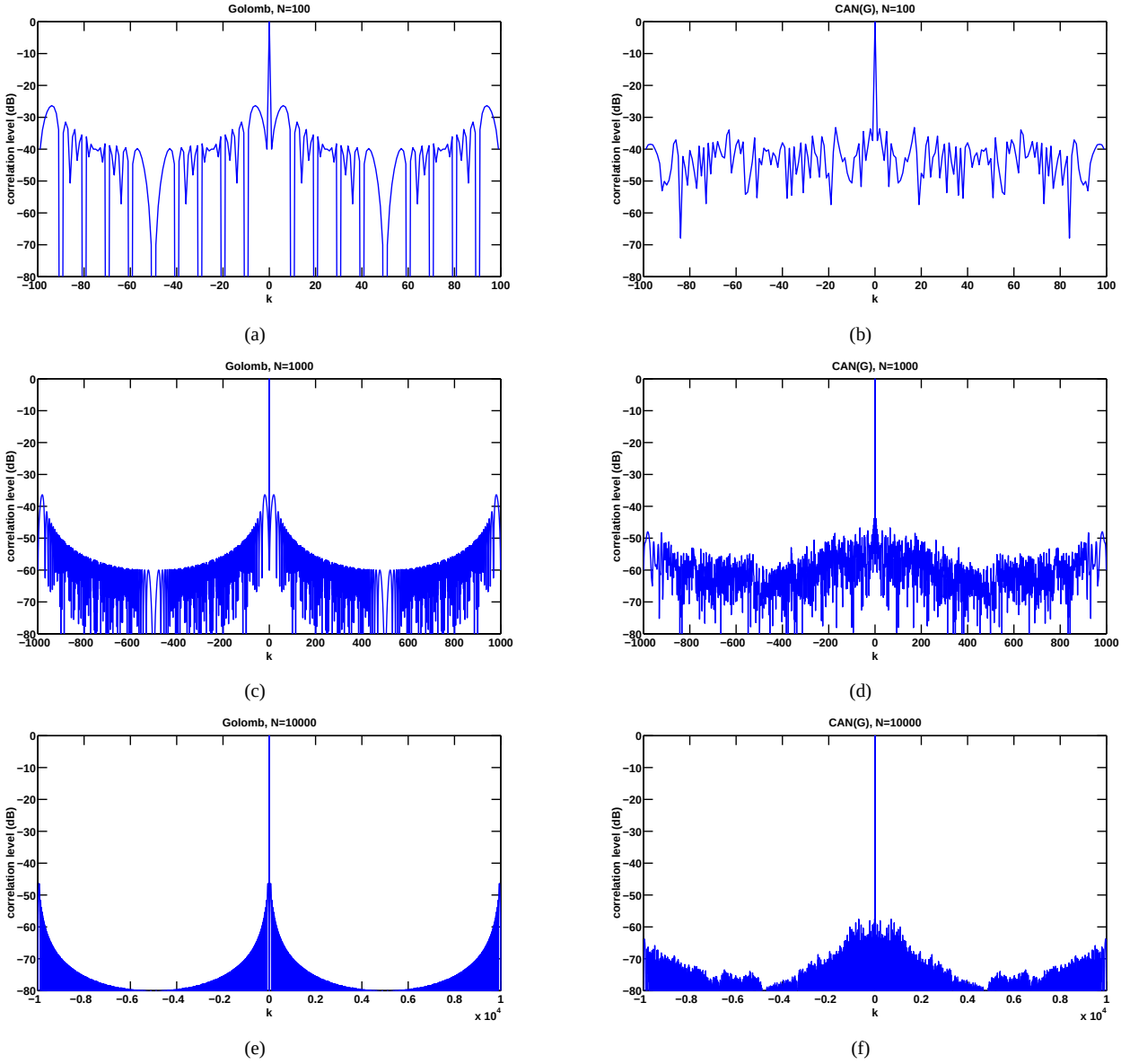

Fig. 2. Correlation levels of the Golomb and CAN sequences of lengths $N = 10^2, 10^3$ and 10^4, designed under the ISL metric. (a) The Golomb sequence, $N = 10^2$, (b) the CAN(G) sequence, $N = 10^2$, (c) the Golomb sequence, $N = 10^3$, (d) the CAN(G) sequence, $N = 10^3$, (e) the Golomb sequence, $N = 10^4$, and (f) the CAN(G) sequence, $N = 10^4$.

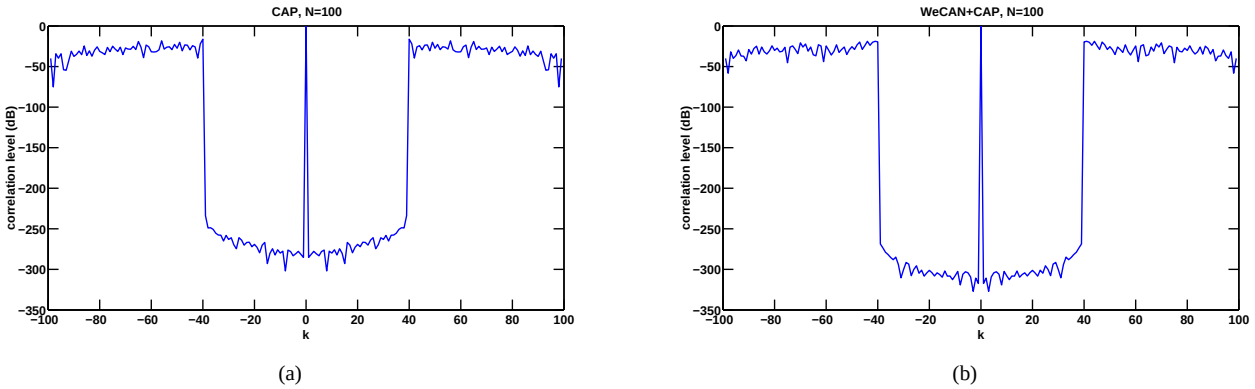

Fig. 4. Correlation levels of the CAP and WeCAN+CAP sequences of length $N = 100$, designed under the WISL metric with weights in Eq. (66). (a) The CAP sequence and (b) the WeCAN+CAP sequence.

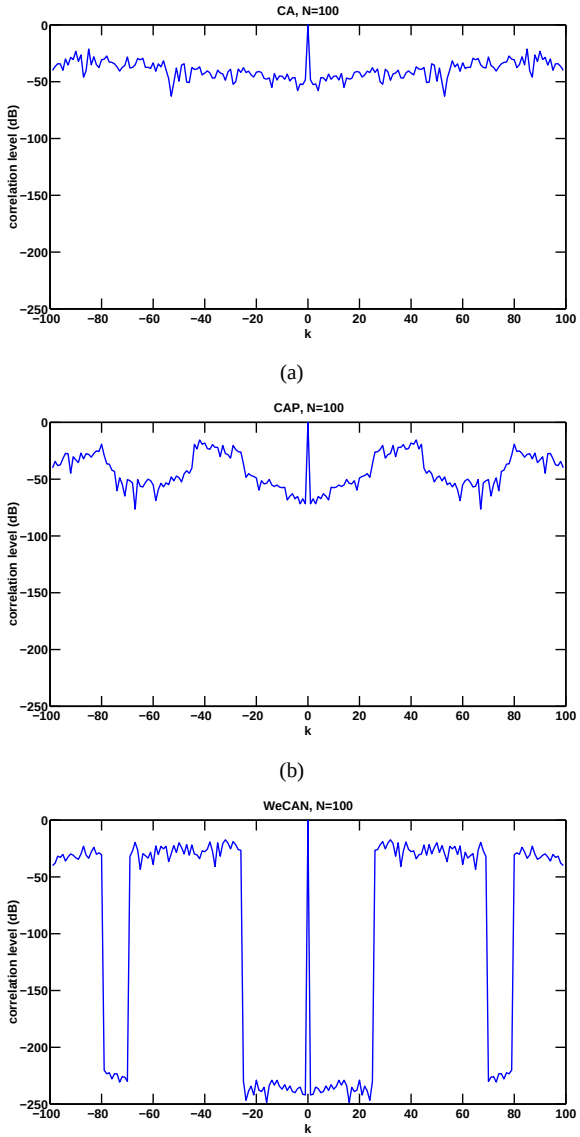

Fig. 3. Correlation levels of the CA, CAP and WeCAN sequences of length $N = 100$. (a) The CA sequence, (b) the CAP sequence and (c) the WeCAN sequence designed under the WISL metric with weights in Eq. (65).

where $\bar{\mathbf{X}}$ is as defined in Eq. (12), and

$$\mathbf{y} = \begin{bmatrix} y_1 & \cdots & y_{N+P-1} \end{bmatrix}^T, \mathbf{h} = \begin{bmatrix} h_0 & \cdots & h_{P-1} \end{bmatrix}^T, \\ \mathbf{e} = \begin{bmatrix} e_1 & \cdots & e_{N+P-1} \end{bmatrix}^T. \quad (69)$$

Let $\bar{\mathbf{x}}_p$ denote the p^{th} column of the matrix $\bar{\mathbf{X}}$. We use $\bar{\mathbf{x}}_p$ as a "matched filter" to determine h_p from $\mathbf{y}$, which leads to the following estimate of h_p:

$$\hat{h}_p = \frac{1}{N} \bar{\mathbf{x}}_p^* \mathbf{y}. \quad (70)$$

Let the number of channel taps be $P = 40$. Figure 5 shows the magnitude of the simulated channel impulse response $\{|h_p|\}_{p=0}^{P-1}$. We perform two experiments to compare the Golomb sequence and the CAP sequence. In one experiment the noise power σ^2 is fixed at 10^{-4} and the sequence length N is varied from 100 to 500; In the other experiment N is fixed at 200 and σ^2 is varied from 10^{-6} to 1. For each pair (N, σ^2), 500 Monte-Carlo trials are run (in which the noise sequence $\mathbf{e}$ is varied) and the mean-squared error (MSE) of $\hat{\mathbf{h}}$ is recorded. Figure 6 shows the MSE of $\hat{\mathbf{h}}$ in the two situations. Due to better autocorrelation properties, the CAP sequence generates consistently smaller MSE than the Golomb sequence. In particular, it is interesting to observe from Figure 6(b) that as σ^2 decreases, the MSE of $\hat{\mathbf{h}}$ corresponding to the CAP sequence is decreasing linearly (and it becomes 0 as σ^2 goes to 0), while the performance of the Golomb sequence is limited to a certain level because of its non-zero correlation sidelobes, which induce an estimation bias.

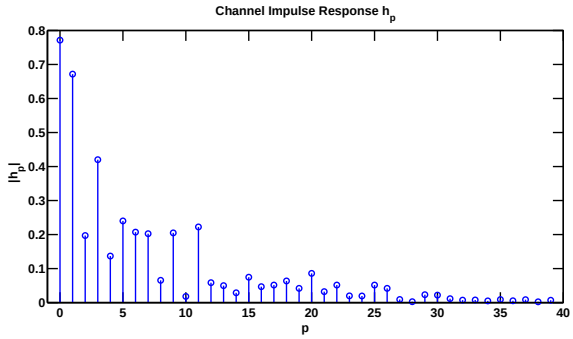

Fig. 5. The magnitude of the simulated channel impulse response $\mathbf{h}$.

VI. Concluding Remarks

We have presented several cyclic algorithms, namely CAP, CAN, WeCAN and WeCAN+CAP which can be used to design unimodular sequences that have good autocorrelation properties. CAN can be used to design very long sequences (of length N up to 10^6), a design problem that can hardly be handled by other algorithms proposed in the previous literature. CAN deals with the ISL metric, i.e., it considers all unweighted correlation lags from r_1 up to r_{N-1}, whereas CAP, WeCAN and WeCAN+CAP aim to minimize weighted-ISL metrics. We have shown that, in particular, the latter three algorithms can be used to design sequences that have virtually zero autocorrelation sidelobes in a specified lag interval. CAP, WeCAN and WeCAN+CAP can be used to design sequences of lengths $N \sim 10^3$ or larger, depending on how many lags are considered. A number of numerical examples have been provided to demonstrate the good autocorrelation properties of the unimodular sequences designed using the proposed algorithms.

References

[1] J. Jedwab, "A survey of the merit factor problem for binary sequences." *Sequences and Their Applications – SETA 2004*, T. Helleseth, D. Sarwate, H. Y. Song, and K. Yang, Eds. Springer-Verlag, Heidelberg, 2005, vol. 3486, Lecture Notes in Computer Science, pp. 30–55.

[2] T. Høholdt, "The merit factor problem for binary sequences." *Applied Algebra, Algebraic Algorithms and Error-Correcting Codes*, M. Fossorier, H. Imai, S. Lin, and A. Poli, Eds. Springer-Verlag, Heidelberg, 2006, vol. 3857, Lecture Notes in Computer Science, pp. 51–59.

[3] M. J. E. Golay, "Sieves for low autocorrelation binary sequences," *IEEE Transactions on Information Theory*, vol. 23, no. 1, pp. 43–51, January 1977.

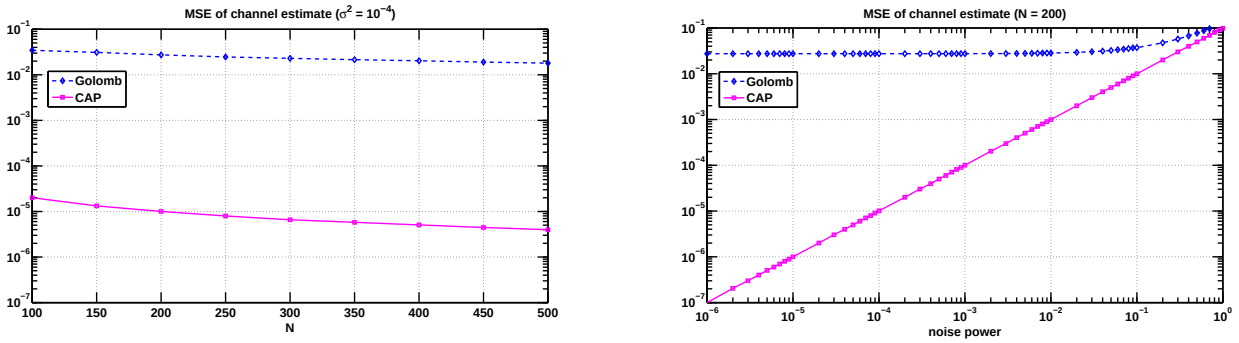

(a) (b)

Fig. 6. The MSE of the estimated $\hat{\mathbf{h}}$ using two training sequences: the Golomb sequence and the WeCAN+CAP sequence. (a) The noise power σ^2 is fixed at 10^{-4} and the sequence length N is varied from 100 to 500; and (b) N is fixed at 200 and σ^2 is varied from 10^{-6} to 1.

[4] J. Lindner, "Binary sequences up to length 40 with best possible autocorrelation function," *Electronics Letters*, vol. 11, no. 21, pp. 507–507, October 1975.

[5] C. D. Groot, D. Würtz, and K. H. Hoffmann, "Low autocorrelation binary sequences: Exact enumeration and optimization by evolutionary strategies," *Optimization*, vol. 23, no. 4, pp. 369–384, 1992.

[6] S. Mertens, "Exhaustive search for low-autocorrelation binary sequences," *J. Phys. A*, vol. 29, pp. 473–481, 1996.

[7] R. Ferguson and J. Knauer, "Optimization methods for binary sequences - the merit factor problem," *MITACS 6th Annual Conference*, University of Calgary, Alberta, Canada, May 2005.

[8] H. D. Schotten and H. D. Lüke, "On the search for low correlated binary sequences," *International Journal of Electronics and Communications*, vol. 59, no. 2, pp. 67–78, 2005.

[9] J. Jedwab, "What can be used instead of a Barker sequence?" *Contemporary Math*, 2008.

[10] T. Xiong and J. Hall, "Construction of even length binary sequences with asymptotic merit factor 6," *IEEE Transactions on Information Theory*, vol. 54, no. 2, pp. 931–935, February 2008.

[11] P. B. Rapajic and R. A. Kennedy, "Merit factor based comparison of new polyphase sequences," *IEEE Communications Letters*, vol. 2, no. 10, pp. 269–270, October 1998.

[12] N. Zhang and S. W. Golomb, "Polyphase sequence with low autocorrelations," *IEEE Transactions on Information Theory*, vol. 39, no. 3, pp. 1085–1089, May 1993.

[13] P. Borwein and R. Ferguson, "Polyphase sequences with low autocorrelation," *IEEE Transactions on Information Theory*, vol. 51, no. 4, pp. 1564–1567, April 2005.

[14] U. Somaini and M. Ackroyd, "Uniform complex codes with low autocorrelation sidelobes (corresp.)," *IEEE Transactions on Information Theory*, vol. 20, no. 5, pp. 689–691, September 1974.

[15] R. Frank, "Polyphase codes with good nonperiodic correlation properties," *IEEE Transactions on Information Theory*, vol. 9, no. 1, pp. 43–45, January 1963.

[16] F. Kretschmer Jr. and K. Gerlach, "Low sidelobe radar waveforms derived from orthogonal matrices," *IEEE Transactions on Aerospace and Electronic Systems*, vol. 27, no. 1, pp. 92–102, January 1991.

[17] H. A. Khan, Y. Zhang, C. Ji, C. J. Stevens, D. J. Edwards, and D. O'Brien, "Optimizing polyphase sequences for orthogonal netted radar," *IEEE Signal Processing Letters*, vol. 13, no. 10, pp. 589–592, October 2006.

[18] J. Benedetto and J. Donatelli, "Ambiguity function and frame-theoretic properties of periodic zero-autocorrelation waveforms," *IEEE Journal of Selected Topics in Signal Processing*, vol. 1, no. 1, pp. 6–20, June 2007.

[19] P. Stoica, J. Li, and X. Zhu, "Waveform synthesis for diversity-based transmit beampattern design," *IEEE Transactions on Signal Processing*, vol. 56, no. 6, pp. 2593–2598, June 2008.

[20] J. A. Tropp, I. S. Dhillon, R. W. Heath, and T. Strohmer, "Designing structured tight frames via an alternating projection method," *IEEE Transactions on Information Theory*, vol. 51, no. 1, pp. 188–209, January 2005.

[21] J. Li, P. Stoica, and X. Zheng, "Signal synthesis and receiver design for MIMO radar imaging," *IEEE Transactions on Signal Processing*, vol. 56, no. 8, pp. 3959–3968, August 2008.

[22] H. He, P. Stoica, and J. Li, "Novel designs of unimodular sequence sets with good correlation – an application to MIMO radar," in preparation.

[23] J. Ling, T. Yardibi, X. Su, H. He, and J. Li, "Enhanced channel estimation and symbol detection for high speed MIMO underwater acoustic communications," *IEEE 13th DSP Workshop & 5th SPE Workshop*, Marco Island, FL, USA, January 2009, to appear.

[24] P. Stoica and R. L. Moses, *Spectral Analysis of Signals*. Upper Saddle River, NJ: Prentice-Hall, 2005.

Petre Stoica (F'94) received the D.Sc. degree in automatic control from the Polytechnic Institute of Bucharest (BPI), Bucharest, Romania, in 1979 and an honorary doctorate degree in science from Uppsala University (UU), Uppsala, Sweden, in 1993.

He is a professor of systems modeling with the Division of Systems and Control, the Department of Information Technology at UU. Previously, he was a professor of system identification and signal processing with the Faculty of Automatic Control and Computers at BPI. He held longer visiting positions with Eindhoven University of Technology, Eindhoven, The Netherlands; Chalmers University of Technology, Gothenburg, Sweden (where he held a Jubilee Visiting Professorship); UU; the University of Florida, Gainesville, FL; and Stanford University, Stanford, CA. His main scientific interests are in the areas of system identification, time series analysis and prediction, statistical signal and array processing, spectral analysis, wireless communications, and radar signal processing.

Dr. Stoica has published nine books, ten book chapters, and some 500 papers in archival journals and conference records. The most recent book he coauthored, with R. Moses, is Spectral Analysis of Signals (Prentice-Hall, 2005). He is on the editorial boards of six journals: the Journal of Forecasting; Signal Processing; Circuits, Signals, and Signal Processing; Digital Signal Processing: A Review Journal; Signal Processing Magazine; and Multidimensional Systems and Signal Processing. He was a co-guest editor for several special issues on system identification, signal processing, spectral analysis, and radar for some of the aforementioned journals, as well as for IEE Proceedings. He was corecipient of the IEEE ASSP Senior Award for a paper on statistical aspects of array signal processing. He was also recipient of the Technical Achievement Award of the IEEE Signal Processing Society. In 1998, he was the recipient of a Senior Individual Grant Award of the Swedish Foundation for Strategic Research. He was also co-recipient of the 1998 EURASIP Best Paper Award for Signal Processing for a work on parameter estimation of exponential signals with time-varying amplitude, a 1999 IEEE Signal Processing Society Best Paper Award for a paper on parameter and rank estimation of reduced-rank regression, a 2000 IEEE Third Millennium Medal, and the 2000 W. R. G. Baker Prize Paper Award for a paper on maximum likelihood methods for radar. He was a member of the international program committees of many topical conferences. From 1981 to 1986, he was a Director of the International Time-Series Analysis and Forecasting Society, and he was also a member of the IFAC Technical Committee on Modeling, Identification, and Signal Processing. He is also a member of the Royal Swedish Academy of Engineering Sciences, an honorary member of the Romanian Academy, and a fellow of the Royal Statistical Society.

Jian Li (S'87-M'91-SM'97-F'05) received the M.Sc. and Ph.D. degrees in electrical engineering from The Ohio State University, Columbus, in 1987 and 1991, respectively.

From April 1991 to June 1991, she was an Adjunct Assistant Professor with the Department of Electrical Engineering, The Ohio State University, Columbus. From July 1991 to June 1993, she was an Assistant Professor with the Department of Electrical Engineering, University of Kentucky, Lexington. Since August 1993, she has been with the Department of Electrical and Computer Engineering, University of Florida, Gainesville, where she is currently a Professor. In Fall 2007, she was on sabbatical leave at MIT, Cambridge, Massachusetts. Her current research interests include spectral estimation, statistical and array signal processing, and their applications.

Dr. Li is a Fellow of IEEE and a Fellow of IET. She is a member of Sigma Xi and Phi Kappa Phi. She received the 1994 National Science Foundation Young Investigator Award and the 1996 Office of Naval Research Young Investigator Award. She was an Executive Committee Member of the 2002 International Conference on Acoustics, Speech, and Signal Processing, Orlando, Florida, May 2002. She was an Associate Editor of the IEEE Transactions on Signal Processing from 1999 to 2005, an Associate Editor of the IEEE Signal Processing Magazine from 2003 to 2005, and a member of the Editorial Board of Signal Processing, a publication of the European Association for Signal Processing (EURASIP), from 2005 to 2007. She has been a member of the Editorial Board of Digital Signal Processing – A Review Journal, a publication of Elsevier, since 2006. She is presently a member of the Sensor Array and Multichannel (SAM) Technical Committee of IEEE Signal Processing Society. She is a co-author of the papers that have received the First and Second Place Best Student Paper Awards, respectively, at the 2005 and 2007 Annual Asilomar Conferences on Signals, Systems, and Computers in Pacific Grove, California. She is also a co-author of the paper that has received the M. Barry Carlton Award for the best paper published in IEEE Transactions on Aerospace and Electronic Systems in 2005.

Hao He (S'08) received the B.Sc. degree in electrical engineering from the University of Science and Technology of China (USTC), Hefei, China, in 2007. He is currently pursuing the Ph.D. degree with the Department of Electrical Engineering at University of Florida, Gainesville, FL, USA.

His research interests are in the areas of spectral estimation and radar signal processing.